Jikeikai Med J 2021 ; 68 : 67-79

The Role of Tenascin C during the Development of DSS Induced Colitis

Atsushi HOSHINO[1,2,3#], Hiroki SAIJO[2#], Norifumi TATSUMI[2], Seiji ARIHIRO[1], Masataka OKABE[2], Masayuki SARUTA[1], Moriaki KUSAKABE[3], and Hisashi HASHIMOTO[2]

[1]*Division of Gastroenterology and Hepatology, Department of Internal Medicine, The Jikei University School of Medicine*
[2]*Department of Anatomy, The Jikei University School of Medicine*
[3]*Research Center for Food Safety, Graduate School of Agricultural and Life Sciences, The University of Tokyo*

ABSTRACT

Ulcerative colitis is a chronic inflammatory bowel disease of unknown etiology. In this study, we examined the distribution and role of tenascin C (TNC) in the colitis induced by dextran sulfate sodium (DSS) in a mouse, an experimental model of ulcerative colitis. During the development of DSS-induced colitis, chronological changes of the mucosa, TNC expression, distribution of hypoxia inducible factor-1α positive cells, and vascular networks were investigated, and also TNC-producing cells were detected by *in situ* hybridization. Furthermore, the amounts of vascular endothelial growth factor A and albumin in the mucosa and of messenger RNA of TNC, tumor necrosis factor α and interleukin 6 were examined. The expression of TNC was weak and confined to the lamina propria just beneath the mucosal epithelium in the control mouse, and increased and expanded to the deep part of the lamina propria with the progression of DSS-induced colitis. The distribution of TNC resembled that of temporarily stretched cryptal cells and of hypoxia-inducible factor 1α-positive cells. Expression levels of interleukin 6 and tumor necrosis factor α were increased before TNC. These results suggest that TNC is induced by hypoxia, tensile stress, and inflammatory cytokines to support the epithelium and to reduce excessive inflammation.

(Jikeikai Med J 2021 ; 68 : 67-79)

Key words : ulcerative colitis, dextran sulfate sodium, tenascin C, hypoxia-inducible factor 1 alpha, inflammatory cytokines

INTRODUCTION

Ulcerative colitis (UC), along with Crohn's disease, is a chronic inflammatory bowel disease that causes idiopathic inflammation of the gastrointestinal tract and requires long-term treatment owing to repeated relapse and remission in more than half of patients[1]. Although the precise etiology of UC is unknown, disrupted intestinal mucosal barrier function has been implicated in the pathogenesis[2,3]. Invasion of an antigen, such as the intestinal bacteria, into the lamina propria generates an excessive immune response and continuing mucosal injury[4]. In studies of dextran sulfate sodium (DSS)-induced colitis in mice, which is a representative animal model of UC, various mechanisms of the pathogenesis have been reported[5-7]. We have proposed that local hypoxia due to disturbances in the mucosal microcirculation damag-

Received : March 15, 2021 / Accepted : March 19, 2021
星野　優，西條　広起，辰巳　徳史，有廣　誠二，岡部　正隆，猿田　雅之，日下部守昭，橋本　尚詞
Mailing address : Hisashi HASHIMOTO, Department of Anatomy, The Jikei University School of Medicine, 3-25-8 Nishi-shimbashi, Minato-ku, Tokyo 105-8461, Japan.
E-mail : hashimoto.anat@jikei.ac.jp
#equally contributed

es the mucosal and cryptal epithelium and triggers the inflammatory response[8]. Subsequently, inflammatory cells, which secrete inflammatory cytokines, such as interleukin (IL)-1β, IL-6, and tumor necrosis factor (TNF)-α, would infiltrate the lamina propria and aggravate inflammation[9].

Diverse functions of the mucosal epithelial cells, including their turnover, contribute to the barrier function of the mucosa. Mucosal epithelium is constantly attacked by digestive enzymes and intestinal bacteria, but it does not easily exfoliate and can continue to maintain its functions. The homeostasis of mucosal epithelium is considered to be maintained by interaction with the interstitium. We have hypothesized that if the interstitium is unable to support the epithelium, the epithelial cells would be continuously injured by slight stimulation and the inflammation would be manifested. Therefore, analyzing how the mucosal epithelium and the interstitium are related might reveal the intestinal mucosal barrier mechanism.

Of the various constituents of the interstitium, we have focused on an extracellular matrix glycoprotein, tenascin C (TNC). Although highly expressed during embryogenesis, TNC is hardly present in normal adult tissue but rapidly reappears in various pathological conditions, including oncogenesis and wound healing[10,11]. In an experiment to induce colitis by DSS administration to both wild-type TNC(+/+) and the TNC null TNC(−/−) BALB/cA mice, severe colitis was induced in TNC null mice, even at a DSS concentration that did not cause colitis in wild-type mice[12]. Furthermore, TNC may make stromal cells exert their functions during inflammation and wound healing process, and in the regulation of inflammation[13,14].

In the present study, we examined the relationships between mucosal epithelium and the interstitium and between the interaction of TNC and cytokines, to clarify intestinal mucosal barrier function. In mice with DSS-induced colitis, chronological changes in TNC expression, the distribution of hypoxia-inducible factor 1 alpha (HIF-1α)-positive cells, and vascular networks were investigated with a laser scanning microscope, and TNC-producing cells were investigated by *in situ* hybridization for TNC messenger RNA (mRNA). We also examined the amounts of vascular endothelial growth factor A (VEGF-A) and albumin in the mucosa and the amounts of mRNA of TNC and inflammatory cytokines, TNF-α, and IL-6.

Materials and Methods

Animals and experimental design

Male C57BL/6J mice (9 to 10 weeks old) were housed under conventional conditions. The animal experiments were approved by the Institutional Animal Care and Use Committee of The Jikei University School of Medicine (Approval Number 2015-140) and performed under the guidelines of The Jikei University School of Medicine Animal Research Facility. The colitis was induced in the mice by replacing drinking water with 2.0% (wt/vol) DSS (36 to 50 kDa ; MP Biomedicals, Tokyo, Japan) in tap water for 7 days[5]. The DSS-administered mice were euthanized on days 0, 3, 5, and 7 and evaluated. Characteristic findings observed in the mice of each experimental day were presented.

Histological assessment of colitis

Histological assessment of colitis was performed as described previously[8]. In short, mice were perfused with a fixative consisting of 4% paraformaldehyde in sodium phosphate buffer (SPB, pH 7.4) under deep anesthesia with sodium pentobarbital. The colon was removed, slit open with scissors, and rolled up around a wooden stick to prepare the Swiss-roll[15]. The specimen was further fixed in the same fixative, embedded in paraffin, and sliced at a thickness of 4 μm with a sliding microtome. The paraffin section was stained with hematoxylin and eosin for histological observations, or stained by the immunohistochemical method described below.

To assess the effect of DSS administration on the cryptal epithelium, the width of cryptal cells was estimated on days 0 and 3. Thirty crypts were randomly selected on a section of the distal colon. The length of each crypt was measured, and the number of cryptal cell nuclei in the crypt was counted. The width of a cryptal cell was calculated by multiplying the length of a crypt by two and then dividing by the number of cryptal cell nuclei in the crypt.

Antibodies

The following primary and secondary antibodies were used : rabbit anti-Ki67 polyclonal antibody (1/2,000 dilution ; ab15580 ; Abcam, Tokyo, Japan), rat anti-TNC monoclonal antibody (clone 3-6 ; 1/1,000 dilution)[16], rabbit anti-HIF-1α polyclonal antibody (1/100 dilution ; NB

100-479 ; Novus Biologicals, LCC, Centennial, CO, USA), rat anti-F4/80 monoclonal antibody (1/2,000 dilution ; ab6640 ; Abcam), rabbit anti-E-cadherin monoclonal antibody (clone 24E10 ; 1/200 dilution ; 3195s ; Cell Signaling Technology, Tokyo, Japan), mouse anti-VEGF-A monoclonal antibody (clone VG-1;1/1,000 dilution ; ab1316 ; Abcam), rabbit anti-albumin polyclonal antibody (1/1,000 dilution ; RARa/Alb/7S ; Nordic Immunological Laboratories, Tilburg, the Netherlands), mouse anti-β actin monoclonal antibody (clone C4 ; 1/1,000 dilution ; sc-47778 ; Santa Cruz Biotechnology, Dallas, TX, USA), biotinylated goat anti-rabbit IgG antibody (1/200 dilution ; BA-1000 ; Vector Laboratories, Burlingame, CA, USA), biotinylated goat anti-rat IgG antibody (1/500 dilution ; 112-065-167 ; Jackson ImmunoResearch Laboratories, West Grove, PA, USA), Alexa Fluor® 488-conjugated goat anti-rat IgG antibody (1/500 dilution ; A-11006 ; Life Technologies, Tokyo, Japan), Alexa Fluor® 633-conjugated goat anti-rabbit IgG antibody (1/500 dilution ; A-21070 ; Life Technologies), horseradish peroxidase (HRP)-conjugated donkey anti-rabbit IgG antibody (1/10,000 dilution ; NA934-100UL ; GE Healthcare, Tokyo, Japan), and HRP-conjugated sheep anti-mouse IgG antibody (1/10,000 dilution ; NA931-100UL ; GE Healthcare).

Immunohistochemistry for Ki67, TNC, and HIF-1α on paraffin sections

An immunohistochemical examination of Ki67 on the paraffin section was performed as described previously[8]. For TNC detection, the paraffin section underwent the same processes as for Ki67 detection except the antigen retrieval step with a citrate buffer. For F4/80 detection, the antigen retrieval step was performed with proteinase K instead of the citrate buffer. Briefly, proteinase K (25530049 ; Thermo Fisher Scientific, Tokyo, Japan) was dissolved in 50 mM Tris-EDTA buffer, pH 8.0, at a concentration of 20 μg/mL. Deparaffinized sections were covered with the proteinase K solution and incubated for 3 minutes at room temperature.

Double immunofluorescence staining for TNC and HIF-1α was performed on paraffin sections. A rat anti-TNC monoclonal antibody and a rabbit anti-HIF-1α polyclonal antibody were used as the primary antibodies. An Alexa Fluor® 488-conjugated goat anti-rat IgG antibody and an Alexa Fluor® 633-conjugated goat anti-rabbit IgG antibody were used as the secondary antibodies. For nuclei staining, 4',6-diamido-2-phenylindole (DAPI, D9542 ; Sigma-Aldrich Japan K.K., Tokyo, Japan) solution at a concentration of 0.1 μg/mL in 0.01 M phosphate-buffered saline (PBS), pH 7.2, was used. The sections were mounted with a mounting medium consisted of 0.05 M Tris-HCl-buffered saline (pH 8.0) containing 90% (vol/vol) nonfluorescent glycerin and 10 mg/mL of 1,4-diazabicyclo[2.2.2]octane (DABCO) and were observed with a confocal laser scanning microscope (LSM-880, Carl Zeiss AG, Oberkochen, Germany).

Vascular cast with rhodamine isothiocyanate-labeled gelatin, preparation of thick sections, and double immunofluorescence staining for TNC and E-cadherin

A vascular cast of the colon with rhodamine isothiocyanate (RITC)-labeled gelatin was obtained, and double immunofluorescence staining of thick sections was performed as described previously[8]. In short, RITC-labeled gelatin was prepared by labeling gelatin (gelatin RR ; Aibis Inc., Osaka, Japan) with RITC (R1755, Sigma-Aldrich Japan K.K.). At the time of euthanasia, the mice under deep anesthesia with sodium pentobarbital were perfused with the warm 10% RITC-labeled gelatin solution. After perfusion, the mice were immersed immediately in a chilled fixative consisting of 0.5% paraformaldehyde and 15% (vol/vol) of a saturated picric acid solution in SPB to gel the RITC-gelatin solution. Then, the colon was carefully removed and further fixed in the same fixative at 4°C. The colon was rinsed with PBS, and thick frozen sections were made at a thickness of 100 μm. The thick sections were pretreated with 3% aqueous solution of sodium deoxycholate and incubated with a mixture of a rat anti-TNC monoclonal antibody and a rabbit anti-E-cadherin monoclonal antibody. After several rinses with PBS, the sections were incubated with a mixture of an Alexa Fluor® 488-conjugated goat anti-rat IgG antibody and an Alexa Fluor® 633-conjugated goat anti-rabbit IgG antibody. The thick sections were mounted and observed as stated above.

Western blot analysis of albumin and VEGF-A

Western blot analysis was performed as described previously[8]. At the time of euthanasia, mice under deep anesthesia with sodium pentobarbital were perfused with cold PBS. The distal colon was removed and homogenized in a lysis buffer (0.05 M Tris-HCl, pH 7.4 ; 0.1 M NaCl ; and

1% Triton X-100) containing complete protease inhibitors (4693116 ; Roche Diagnostics, Tokyo, Japan). The supernatant was collected and assayed for protein concentration with a BCA Protein Assay Kit (23225 ; Thermo Fisher Scientific). The protein concentration in each supernatant was adjusted to 5 mg/mL with the lysis buffer. One milliliter of each supernatant was mixed with 950 μL of Laemmli's sample buffer (161-0737 ; Bio-Rad Laboratories, Tokyo, Japan) and 50 μL of 2-mercaptoethanol and incubated at 95°C for 10 minutes. Each mixture was subjected to 15% sodium dodecyl sulfate-polyacrylamide gel electrophoresis (SDS-PAGE). After electrophoresis, proteins in the gel were electrotransferred to a Hybond-P polyvinylidene difluoride (PVDF) membrane (2322450 ; Atto Corp., Tokyo, Japan). The membrane was incubated with a rabbit anti-albumin polyclonal antibody and a mouse anti-VEGF-A monoclonal antibody, or with a mouse anti-β-actin antibody as the primary antibodies. Then, the membrane was incubated with the HRP-conjugated antibodies (anti-rabbit IgG and anti-mouse IgG) as the secondary antibodies. The immunoreaction was detected with a chemiluminescence ECL Prime Western Blotting Detection Reagent (72-AS01-21 ; GE Healthcare) and a ChemiDoc XRS+gel imaging system (170-8265J2PC ; Bio-Rad Laboratories).

Tissue preparation for in situ hybridization

Tissue preparation for *in situ* hybridization was performed as described previously[8]. The colon was obtained from mice perfused with 4% paraformaldehyde in SPB, sliced transversely with razor blades, and further fixed in the same fixative at 4°C overnight. Then, the specimen was rinsed with cold PBS, and cryosections were obtained at a thickness of 10 μm with a cryostat (CM3050S ; Leica, Tokyo, Japan).

Isolation of complementary DNA encoding the tenascin C gene

To isolate the tenascin C gene (*Tnc*), total RNA was extracted from the colon of a wild-type mouse with TRIzol Reagent (15596-026 ; Life Technologies, Tokyo, Japan). First-strand complementary DNAs were reverse transcribed with a PrimeScript II 1st strand cDNA Synthesis Kit (6210A ; Takara Bio, Tokyo, Japan). A primer pair (forward primer, 5'-CCATGGGTTCTCCGAAGGAA -3' ; reverse primer, 5'-GTCACCTGCTGTTCCACTG-3')[17] specific for *Tnc* was used. The polymerase chain reaction (PCR) with a DNA polymerase (Blend Taq -Plus-, BTQ-201 ; Toyobo, Osaka, Japan) was performed under the following conditions : 95°C for 30 seconds, and 30 cycles of 55°C for 30 seconds and 72°C for 1 minute. The PCR products were ligated into pGEM-T Easy Vector plasmids (A1360 ; Promega, Tokyo, Japan) and sequenced.

In situ hybridization for Tnc

A digoxigenin-labeled antisense RNA probe was synthesized with a DIG RNA Labeling Kit (T7, 1175025 ; Roche Diagnostics) with the plasmids containing the TNC gene. *In situ* hybridization for *Tnc* was performed with a method reported previously[18].

Real-Time quantitative reverse transcriptase-PCR analysis

Total RNA extraction, cDNA synthesis and quantitative reverse transcription (qRT)-PCR were performed as described previously[8]. Used for PCR assay were specific primer sets for *Tnc* (forward 5'-ACCATGCTGAGATAGATGTTCCAAA-3' ; reverse 5'-CTTGACAGCAGAAACACCAATCC-3')[19], for the interleukin 6 (*Il6*) gene (forward 5'-GACAAAGCCAGAGTCCTTCAGAGA-3' ; reverse 5'-CTAGGTTTGCCGAGTAGATCTC-3')[20], for the tumor necrosis factor (*Tnfa*) gene (forward 5'-ACGGCATGGATCTCAAAGAC-3' ; reverse 5'-CGGACTCCGCAAAGTCTAAG-3')[12], and for the actin, beta (*Actb*) gene (β-actin, forward 5'-CAACGGCTCCGGCATGTGC-3' ; reverse 5'-CTCTTGCTCTGGGCCTCG-3')[21].

Total RNA was isolated from the distal colon with TRIzol Reagent and followed by DNase treatment (DNase I, Amplification Grade, 18068-015 ; Life Technologies) to avoid contaminating genomic DNA. Total RNA (1.0 μg) was reverse transcribed with a PrimeScript II 1st strand cDNA Synthesis Kit, and SYBR green-based Real-Time qRT-PCR was performed with SYBR Select Master Mix (4472908 ; Life Technologies).

Statistical analysis

Results are presented as mean ± s.e.m. Student's *t*-test was used for comparison between groups. Steel's multiple comparison test was used to compare among multiple groups. The *P*-values of <0.05 were regarded as significant.

Results

Pathological changes of colonic mucosa in DSS-induced colitis

On day 0 (Fig. 1A), the colon was lined with the columnar epithelium and had deep crypts arriving at the muscularis mucosae. The lamina propria consisted of a loose connective tissue containing a few smooth muscle cells and migrating cells. Cells immunopositive for Ki67 were found at the bottom of crypts and in the lamina propria. Expression of TNC was restricted to the surroundings of the small blood vessels in the lamina propria just beneath the mucosal epithelium.

On day 3 (Fig. 1A), the crypts became distorted but still extended as far as the muscularis mucosae. A decrease in the number of cryptal cells in a crypt caused a significant increase in the width of cryptal cells from day 0 to day 3 (Fig. 1B, $*P<0.05$). Both the number of Ki67-positive cells in the crypts and their immunoreactivity was greatly decreased. However, the number of Ki67-positive cells in the lamina propria remained unchanged. The expression of TNC spread downward from the upper layer of the lamina

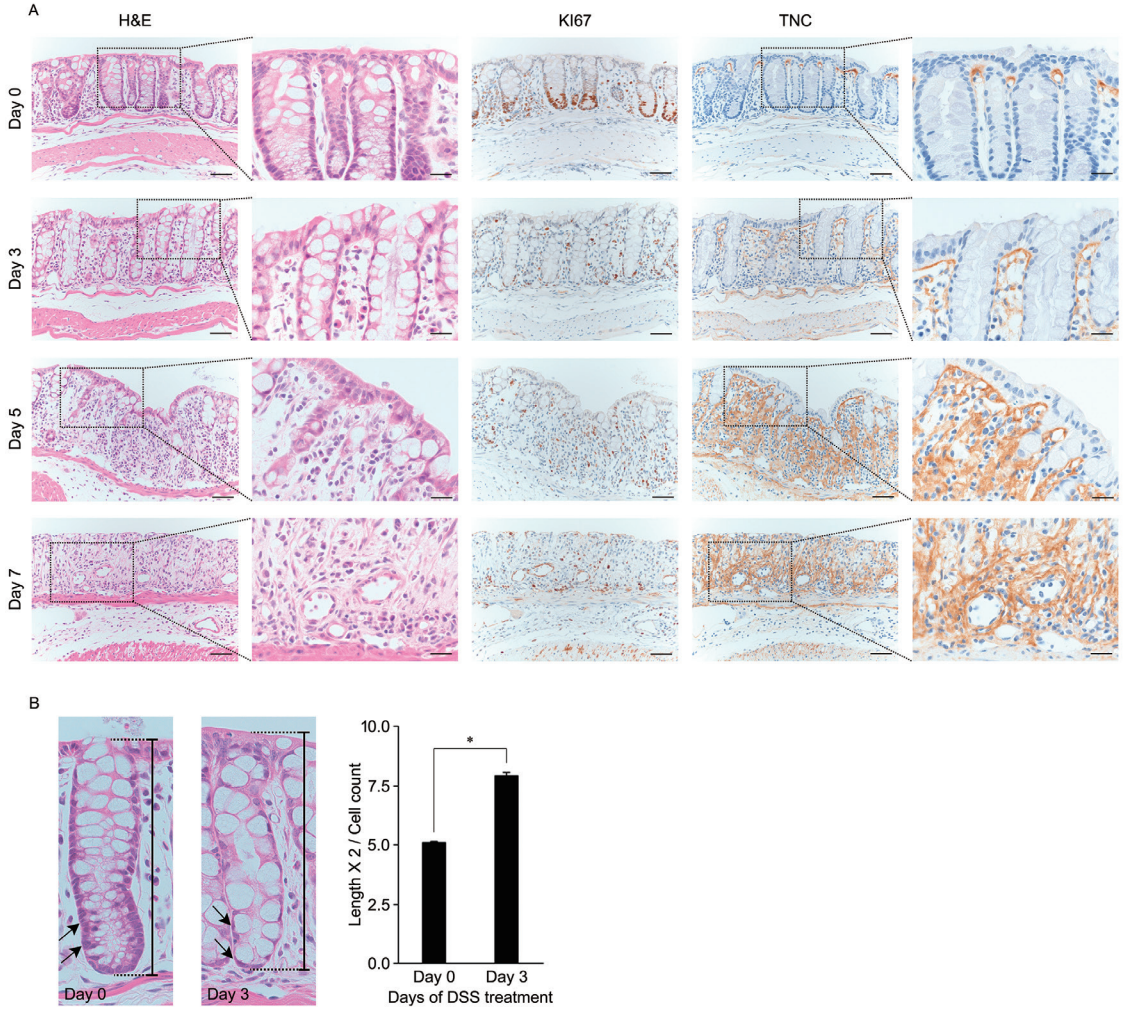

Fig. 1. Dextran sulfate sodium (DSS) administration diminishes cell division in the proliferative zone of crypts and increases tenascin C (TNC) expression.
(A) Serial paraffin sections of the distal colon from DSS-administered mice, stained with hematoxylin and eosin, and stained immunohistochemically for Ki67 and TNC. Scale bars : 50 μm (low-power field) and 20 μm (high-power field). With the progression of DSS-induced colitis, immunoreaction for Ki67 is diminished in crypts and becomes conspicuous in the lamina propria. Immunoreaction for TNC spreads from the upper part to the deep part of the lamina propria.
(B) Decrease in the number of cryptal cells in a crypt causes a significant increase in the width of the cryptal cells between day 0 and day 3 ($*P < 0.05$).

propria to the middle layer along the crypts.

On day 5 (Fig. 1A), the crypts had been shortened or lost, and the number of goblet cells was much lower than on day 3. Inflammatory cells had increased in the lamina propria and infiltrated the submucosa. No Ki67-positive cells were found in the mucosal and cryptal epithelium, whereas many inflammatory cells in the lamina propria showed immunoreactivity for Ki67. Immunoreactive TNC was found through the lamina propria and had spread to the submucosa beyond the muscularis mucosae.

On day 7 (Fig. 1A), the mucosal epithelium was completely lost, and inflammatory cells had increased in the lamina propria and the submucosa. Cells positive for Ki67 were conspicuous in the lamina propria. The TNC was distributed throughout the lamina propria and was strongly expressed around dilated blood vessels in its deep layer.

The relationship between TNC expression and vascular permeability

Western blot analysis of the colonic mucosal extract revealed that DSS administration had increased the amounts of albumin and VEGF-A protein (Fig. 2A).

On day 0 (Fig. 2B), RITC-gelatin clearly depicted the distribution of blood vessels in the colon. No leakage of RITC-gelatin was found anywhere, including the lamina propria. The TNC was localized around capillaries in the lamina propria just beneath the E-cadherin-positive mucosal epithelium. On day 3 (Fig. 2B), small amounts of RITC-labeled gelatin had leaked sporadically in the colonic mucosa. The leaked RITC-gelatin had spread from the deep layer to the surface layer of the lamina propria. In accordance with the leakage of RITC-gelatin, TNC in the surface layer of the lamina propria increased and had deposited intensely at the basement membrane of the mucosal epithelium and of the upper cryptal epithelium. On day 5 (Fig. 2B), small pieces of E-cadherin-positive mucosal epithelial cells had been exfoliated. The RITC-gelatin had leaked from a blood vessel running just above the muscularis mucosa and spread laterally and to the surface layer of the lamina propria. In contrast, TNC deposition had spread from the surface layer to the deep layer. On day 7 (Fig. 2B), most of the mucosal epithelium in the lesion had exfoliated. Leaked RITC-gelatin had spread throughout the lamina propria and flowed out to the gut lumen. The TNC had decreased in the lamina propria's surface layer but had increased in its deep layer.

Expression of HIF-1α during the development of DSS colitis

Although double immunofluorescence staining of HIF-1α and TNC was performed in this experiment, the distribution of HIF-1α is only described here because findings of TNC distribution were comparable to the above experiments.

On day 0, HIF-1α-positive cells were scattered chiefly in the mucosal epithelium. On day 3, HIF-1α-positive cells had distributed from the mucosal surface to the bottom of crypts. On day 5, the remaining cryptal cells in a reduced crypt, mucosal epithelial cells, and some interstitial cells showed immunoreactivity for HIF-1α. On day 7, only a modest number of cells in the lamina propria showed immunoreactivity for HIF-1α (Fig. 3).

Expression of TNC mRNA on DSS-induced colitis

Hybridization signals of TNC mRNA were found only at the top of the lamina propria on day 0, and at pericryptal regions of the upper lamina propria on day 3. On days 5 and 7, many cells in the lamina propria showed positive signals for TNC mRNA (Fig. 4A). The amount of TNC mRNA in the colonic mucosa on day 3 was similar to that on day 0, and was significantly increased on days 5 and 7, by up to 4-fold (Fig. 4B).

Macrophages and inflammatory cytokines in DSS-induced colitis

In the mucosa of the colon on day 0, few F4/80-positive macrophages were found. On day 3, several F4/80-positive macrophages appeared predominantly in the deeper half of the lamina propria and, on day 5, had increased throughout the lamina propria. On day 7, the F4/80-positive macrophages had further increased and migrated towards the upper lamina propria (Fig. 5A).

The amount of TNF-α mRNA had increased by the administration of DSS. The increase was significant on days 5 and 7 (Fig. 5B). The administration of DSS had greatly increased IL-6 mRNA expression on days 5 and 7 (Fig. 5B).

DISCUSSION

In this study, we investigated changes of the colonic mucosa and the distribution of TNC during the develop-

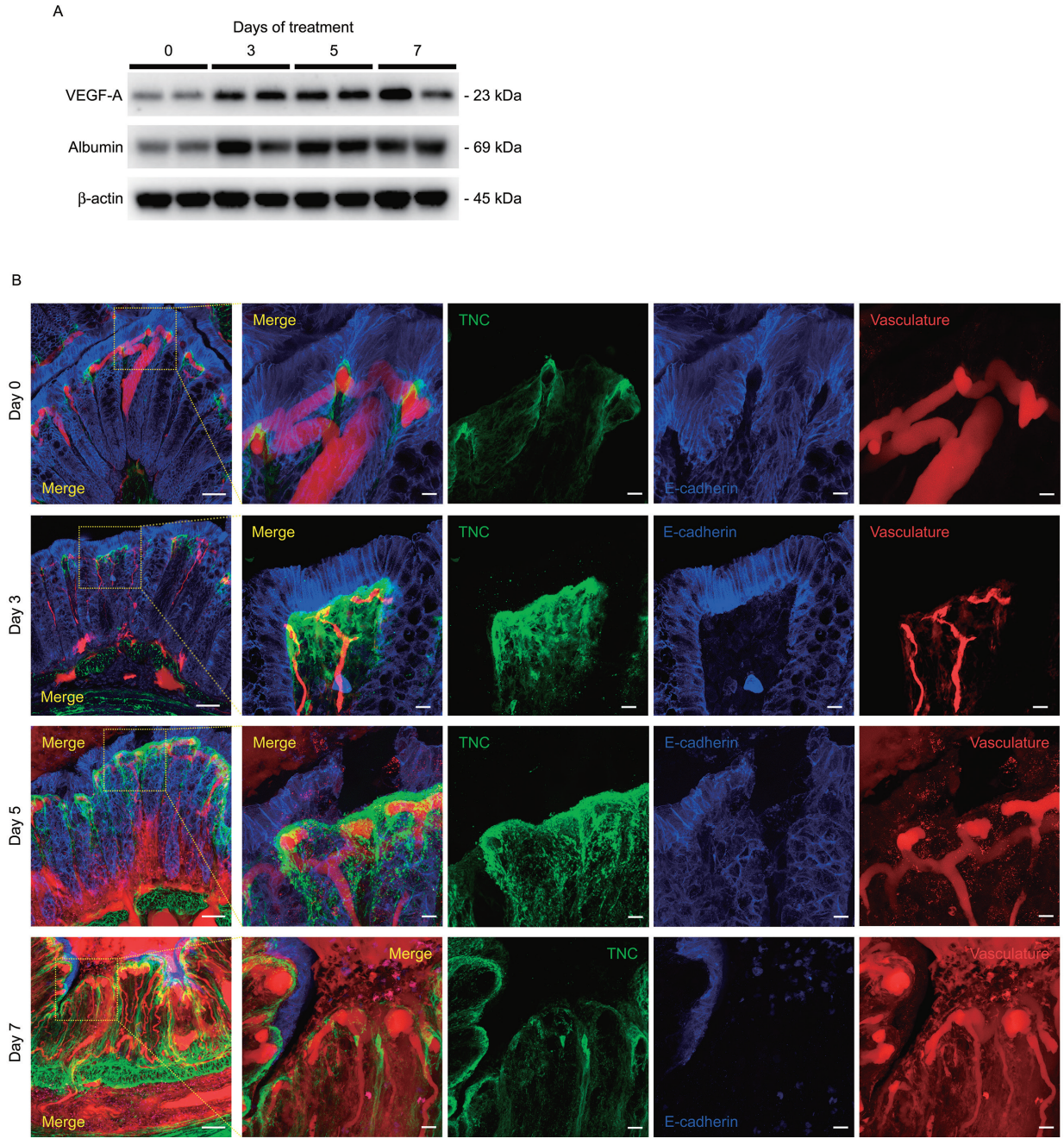

Fig. 2. Dextran sulfate sodium (DSS) administration increases protein levels of vascular endothelial growth factor A (VEGF-A) and albumin in the colonic mucosa, and expands the expression of tenascin C (TNC).
(A) Western blotting images of VEGF-A and albumin in extracts of the mucosa of the distal colon from DSS-administered mice.
(B) Immunofluorescence images for TNC and E-cadherin on 100-μm-thick frozen sections of the distal colon from DSS-administered mice. Scale bars : 50 μm (low-power field) and 10 μm (high-power field). TNC is localized at the surroundings of capillaries just beneath the mucosal epithelium on day 0, conspicuously at the epithelial basement membrane on days 3 and 5, and at the deep part of the lamina propria on day 7. Leaked RITC-gelatin spreads through the lamina propria on days 5 and 7.

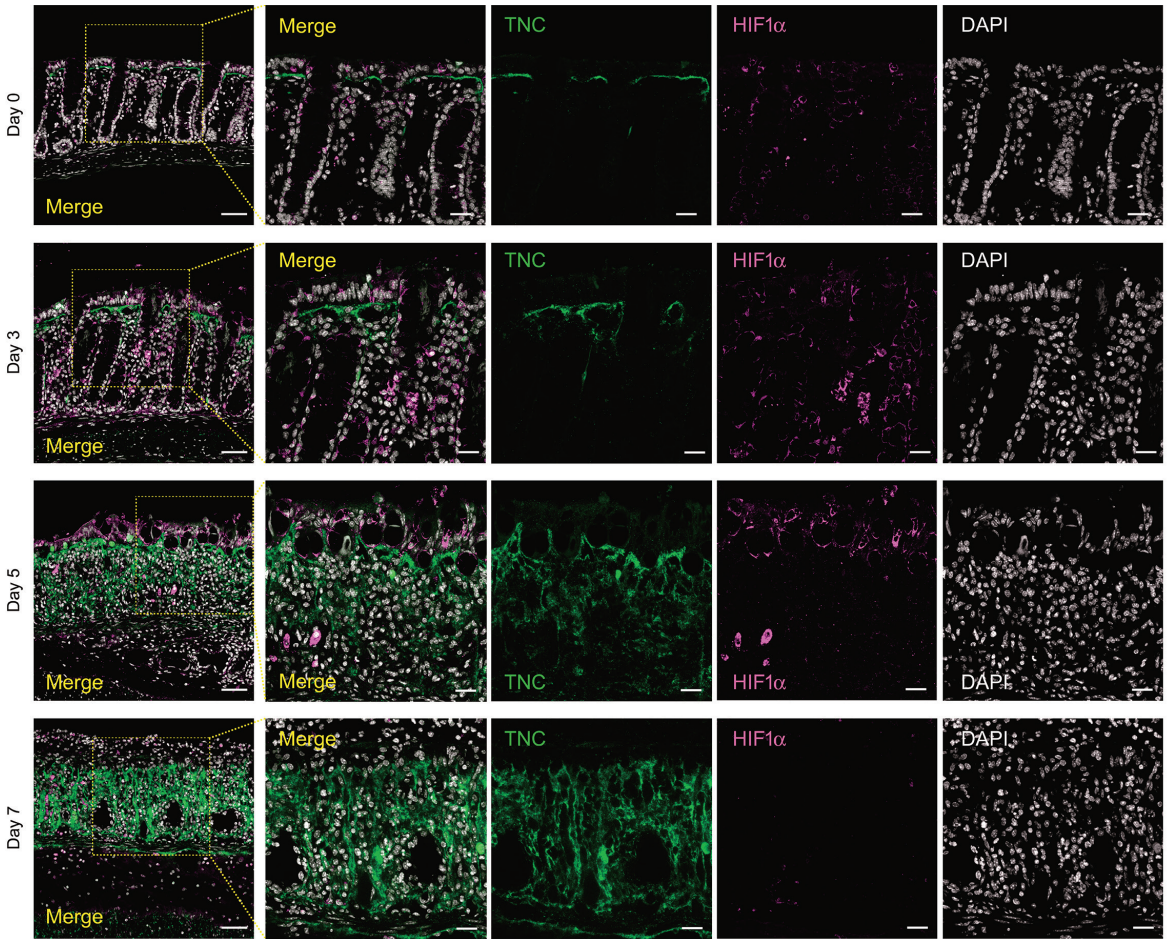

Fig. 3. The expression of hypoxia-inducible factor 1 alpha (HIF-1α) is expanded by dextran sulfate sodium (DSS) administration, and the expansion of HIF-1α distribution is followed by the expression of tenascin C (TNC).
Double immunofluorescence images of and tenascin C (TNC) in the distal colon of the DSS-induced colitis are shown. Scale bars : 50 μm (low-power field) and 20 μm (high-power field). Expression of HIF-1α in the crypt is temporarily up-regulated and expanded by DSS administration, and then gradually decreased as the crypt disintegrates. On day 0, HIF-1α is scattered chiefly in the mucosal epithelium. Many cryptal cells are immunopositive for HIF-1α on day 3. On days 5 and 7, HIF-1α is remarkably expressed in migrating cells in the lamina propria. The distribution of TNC follows that of HIF-1α on days 0 to 5.

ment of DSS-induced colitis to reveal the role of TNC in the barrier function of the colonic mucosa. The present findings are summarized on every experimental day in Table 1 and can be collectively described as follows.

On day 0, the colonic mucosa of normal mice before administering the DSS had deep crypts arriving at the muscularis mucosae, and most cells at the bottom of the crypts were immunopositive for Ki67. Immunopositive TNC and TNC mRNA were present in the lamina propria just beneath the mucosal epithelium. The mucosal epithelial cells expressed HIF-1α. Vascular networks in the mucosa were clearly indicated with RITC-gelatin. Few F4/80-positive macrophages were found in the deep part of the lamina propria.

On day 3 of DSS administration, the histological structure of the mucosa was unchanged except that the number of cryptal cells in crypts was decreased and each cryptal cell was stretched laterally. Immunopositive TNC was slightly increased at the basement membrane of the mucosal epithelium and the upper crypt. Immunoreactivity for HIF-1α had spread throughout the crypt, while the immunoreactivity for Ki67 at the bottom of the crypt was lost. The amounts of VEGF-A and albumin in the mucosa were increased. Leakage of RITC-gelatin into the lamina propria was rarely observed.

On day 5, the crypts were shortened or lost, capillaries

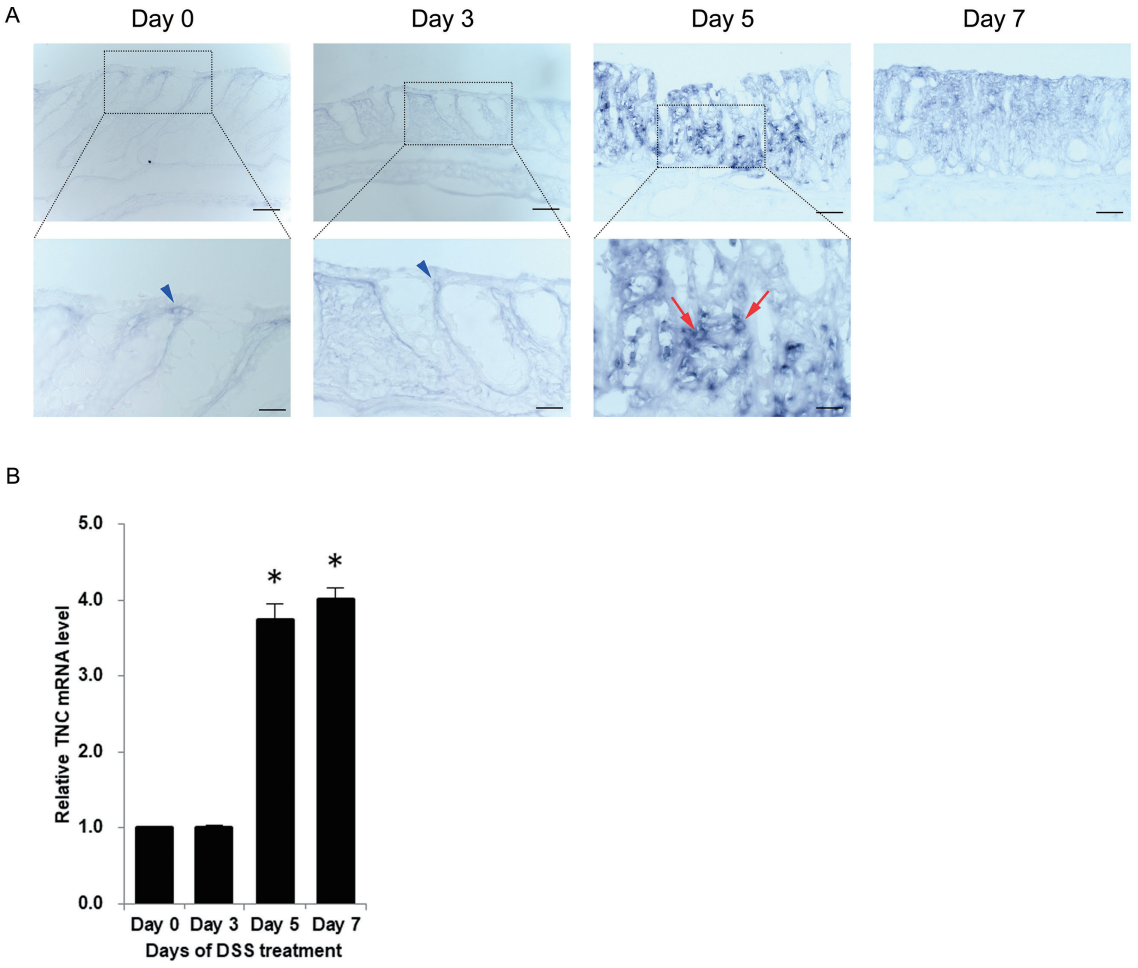

Fig. 4. Dextran sulfate sodium (DSS) administration causes a gradual increase in expression of tenascin C (TNC) mRNA.
(A) *In situ* hybridization for TNC mRNA on frozen sections. Scale bars : 50 μm (low-power field) and 20 μm (high-power field). TNC mRNA is expressed around the lumen located just beneath the mucosal epithelium (arrowheads in A). TNC mRNA positive cells appear in the lamina propria with the progression of DSS-induced colitis (arrows in A).
(B) The expression level of TNC mRNA by real-time quantitative reverse transcription polymerase chain reaction. Significant increases are seen at days 5 and 7. Data are expressed as mean ± s.e.m. ; $n = 5$ each. *$P<0.05$ vs day 0 (wild type).

were dilated and intramural bleeding occurred in the lamina propria. Residual cryptal and mucosal epithelial cells showed immunoreactivity for HIF-1α. Immunopositive TNC had increased and was expressed throughout the lamina propria. The amounts of VEGF-A and albumin in the mucosa were increased. Leaked RITC-gelatin had spread from the deep part to the upper part of the lamina propria. The number of F4/80-positive cells had increased, and expression levels of IL-6 mRNA and TNF-α mRNA had significantly increased.

On day 7, the mucosal epithelium was exfoliated in places, and intraluminal bleeding occurred. Many inflammatory cells had infiltrated throughout the lamina propria, and extravasation of red blood cells had occurred in its depth. Immunoreactivity for HIF-1α had decreased in the remaining epithelial cells ; immunopositive reactions for Ki67 were shown by no epithelial cells but were shown by many migrating cells in the lamina propria. Immunoreactivity for TNC had been intensified in the deep part of the lamina propria but had decreased in its upper part. Leaked RITC-gelatin had spread throughout the lamina propria.

On the basis of these findings, we have made the following hypotheses about the expression and distribution of TNC. The expression of TNC might be facilitated by the hypoxic conditions elicited by disturbances in microcirculation. The expression of HIF-1α in normal mucosal epithelial cells shows that the colonic lumen is generally hypoxic[22]. The distribution of HIF-1α-positive cells was changed in

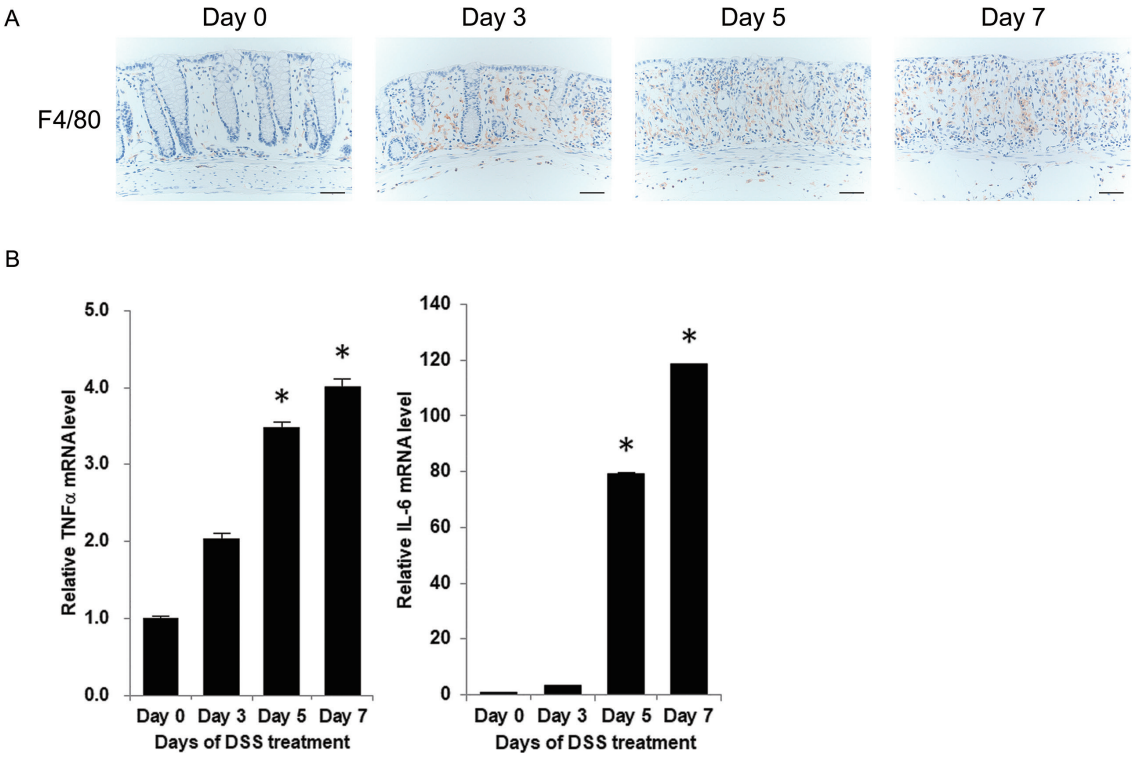

Fig. 5. Dextran sulfate sodium (DSS) administration causes increase in F4/80-positive cells in the lamina propria and in expression levels of tumor necrosis factor (TNF)-α and interleukin (IL) 6 mRNA.
(A) Immunohistochemistry for F4/80 on paraffin sections of the colon of DSS-administered mice. Scare bars : 50 μm. With the progression of DSS-induced colitis, F4/80 positive macrophages increases in the lamina propria.
(B) The expression levels of TNF-α and IL-6 mRNA by real-time quantitative reverse transcription polymerase chain reaction. The administration of DSS causes increases in expressions of TNF-α and IL-6 mRNA, and the increases are significant on days 5 and 7. Data are expressed as mean ± s.e.m. ; $n = 5$ each. *$P<0.05$ vs day 0 (wild type).

the present study by the administration of DSS, indicating that these cells were under hypoxic conditions. On the basis of our previous study, we proposed that DSS-induced colitis is triggered by microcirculatory disturbance in the mucosa[8]. The expression of TNC has been assumed to be induced by hypoxia, reactive oxygen species, and mechanical stress[23]. The expression of TNC has been reported to be modulated by hypoxic conditions with inflammation in synovial fibroblasts in the temporomandibular joint[24]. Furthermore, TNC expression is suggested to be directly regulated by HIF-1α in human glioblastoma cells both *in vitro* and *in vivo*[25]. During the early development of DSS-induced colitis in the present study, the spread of TNC immunoreaction followed that of HIF-1α in the cryptal epithelium. Increases in VEGF-A and albumin in the mucosa due to DSS administration indicates that VEGF-A increased vascular permeability and caused extravasation of albumin[26,27]. Increased vascular permeability and extravasation of plasma might increase interstitial pressure and constrict capillaries. Therefore, hypoxia in the mucosa would be caused by decreased microcirculatory flow. Disturbances in microcirculation cause hypoxic conditions to spread from the upper part to the deep part of the lamina propria, and the expression of TNC is induced.

Another factor that might induce TNC expression is the tensile stress to the mucosal and cryptal epithelium. The administration of DSS stopped both cell division at the bottom of a crypt and the supply of new cells to the crypt. To prevent a change in cryptal length, each cryptal cell and mucosal epithelial cell would be stretched. Sites of TNC induction by tensile stresses found in studies have included the arterial walls of rats in a hypertension model[28], the periosteum of rat ulnae after an external load has been applied[29], and the endomysium after a load has been applied to a skeletal muscle[30]. The expression of TNC has also been reported to be upregulated by the direct tensile stress on fi-

Table 1. Chronological changes to the colon caused by administration of dextran sulfate sodium

	Day 0	Day 3	Day 5	Day 7
Pathological change	none	mild : decrease in crypt goblet cells	moderate : loss of crypts	severe : exfoliation of mucosal epithelium
Ki67-positive cells	in bottom of crypts	decrease in bottom of crypts ↓	in lamina propria ↑	in lamina propria ↑
Tenascin C positivity	surface layer of lamina propria	surface to middle layer of lamina propria	throughout lamina propria	surface layer of lamina propria ↓ ; middle to deep layer of lamina propria ↑
Vascular permeability	none	↑	↑ ↑	↑ ↑
Vascular endothelial growth factor A expression level	low	↑	↑ ↑	↑ ↑
Albumin expression level	low	↑	↑ ↑	↑ ↑
Leakage of rhodamine isothiocyanate gelatin	none	scarcely : bottom of lamina propria	moderate : in deep layer of lamina propria	severe : throughout lamina propria
Hypoxia-inducible factor 1 alpha positivity	in mucosal surface epithelial cells	almost cells of epithelium including the crypt	remaining epithelial cells and some interstitial cells	a few interstitial cells
Tenascin C expression level	low	low	↑	↑ ↑
F4/80-positive cells	a few cells in lamina propria	in lamina propria ↑	in lamina propria ↑ ↑	in lamina propria ↑ ↑
Tumor necrosis factor α expression level	low	slightly increasing ↑	↑	↑ ↑
Interleukin 6 expression level	low	slightly increasing ↑	↑ ↑	↑ ↑ ↑

broblasts *in vivo*[31]. The localization of TNC to the basement membrane of the mucosal and the upper cryptal epithelia reflects the tensile stress to these epithelia.

Furthermore, TNC expression may be induced in response to the inflammatory cytokines, such as IL-6 and TNF-α to suppress inflammation. The TNC knockout mouse has higher expression levels of IL-6 and TNF-α in inflammation than does the wild-type mouse and has tissue injuries that are more severe[32]. A study examining the role of TNC in the DSS-induced colitis using TNC null mice has suggested that disease severity, neutrophil infiltration, and the number of macrophages/monocytes and mRNA levels of the pro-inflammatory cytokines IL-1β and TNF-α are higher in TNC-null mice than in wild-type mice[12]. In addition, TNC plays a protective role against inflammation, and a deficiency of TNC exacerbates asthma and liver fibrosis[13,33,34]. Increases of IL-6 mRNA and TNF-α mRNA expression before the increase of TNC mRNA expression in the present result suggest that inflammatory stimulation to the mucosa by DSS and enterobacteria induce IL-6 and TNF-α expression and that these cytokines induce TNC expression to decrease the inflammatory reaction.

A source of TNC might be macrophages accumulating in excessive inflammation. As inflammation progressed in the present study, the number of F4/80-positive cells was increased in the lamina propria, and the size of these cells was large, indicating that these cells were macrophages. The TNC mRNA-positive cells in the lamina propria would be these macrophages, because human macrophages and a cell line derived from human mononuclear leukocyte U937 express TNC under the regulation of inflammatory cytokines, such as TNF-α and IFN-α[35,36,19]. Thus, IL-6 and TNF-α secreted by macrophages to promote the inflammatory reaction affect macrophages in an autocrine or paracrine manner to secrete TNC to attenuate inflammatory response.

Through this research, TNC expression was induced by the tensile stress on the mucosal and cryptal epithelium and by hypoxia due to microcirculatory disturbance in the early stage of DSS administration. At the later stage, as colitis advances, IL-6 and TNF-α would stimulate macrophages to produce TNC to prevent the inflammatory reaction from progressing.

Finally, TNC expression in human patients with UC must be clarified. By comparing the present findings with TNC expression at the onset and the relapse of UC, it would be helpful to clarify the pathogenesis of the disease, to detect the early inflammation, to maintain the remission,

and to develop novel therapies.

CONFLICT OF INTEREST

Authors have no conflict of interest.

Acknowledgment: This study was supported in part by JSPS KAKENHI Grant Number 25221205, and by Young Scientists Grant Number 19K17414.

REFERENCES

1. Abraham C, Cho JH. Inflammatory bowel disease. N Engl J Med. 2009 ; 361 : 2066–78.
2. Ordás I, Eckmann L, Talamini M, Baumgart DC, Sandborn WJ. Ulcerative colitis. Lancet. 2012 ; 380(9853) : 1606–19.
3. Ramos GP, Papadakis KA. Mechanisms of disease : inflammatory bowel diseases. Mayo Clin Proc. 2019 ; 94 : 155–65.
4. Xavier RJ, Podolsky DK. Unravelling the pathogenesis of inflammatory bowel disease. Nature. 2007 ; 448(7152) : 427–34.
5. Okayasu I, Hatakeyama S, Yamada M, Ohkusa T, Inagaki Y, Nakaya R. A novel method in the induction of reliable experimental acute and chronic ulcerative colitis in mice. Gastroenterology. 1990 ; 98 : 694–702.
6. Elson CO, Sartor RB, Tennyson GS, Riddell RH. Experimental models of inflammatory bowel disease. Gastroenterology. 1995 ; 109 : 1344–67.
7. Kiesler P, Fuss IJ, Strober W. Experimental models of inflammatory bowel diseases. Cell Mol Gastroenterol Hepatol. 2015 ; 1 : 154–70.
8. Saijo H, Tatsumi N, Arihiro S, Kato T, Okabe M, Tajiri H, et al. Microangiopathy triggers, and inducible nitric oxide synthase exacerbates dextran sulfate sodium–induced colitis. Lab Invest. 2015 ; 95 : 728–48.
9. Chassaing B, Aitken JD, Malleshappa M, Vijay-Kumar M. Dextran sulfate sodium (DSS)–induced colitis in mice. Curr Protoc Immunol. 2014 ; 104 : 15.25.1–15.25.14.
10. Chiquet-Ehrismann R, Mackie EJ, Pearson CA, Sakakura T. Tenascin : an extracellular matrix protein involved in tissue interactions during fetal development and oncogenesis. Cell. 1986 ; 47 : 131–9.
11. Sumioka T, Kitano A, Flanders KC, Okada Y, Yamanaka O, Fujita N, et al. Impaired cornea wound healing in a tenascin C–deficient mouse model. Lab invest. 2013 ; 93 : 207–7.
12. Islam MS, Kusakabe M, Horiguchi K, Lino S, Nakamura T, Iwanaga K, et al. PDGF and TGF-β promote tenascin-C expression in subepithelial myofibroblasts and contribute to intestinal mucosal protection in mice. Br J Pharmacol. 2014 ; 171 : 375–88.
13. Nakao N, Hiraiwa N, Yoshiki A, Ike F, Kusakabe M. Tenascin-C promotes healing of habu–snake venom–induced glomerulonephritis : studies in knockout congenic mice and in culture. Am J Pathol. 1998 ; 152 : 1237–45.
14. Matsuda A, Hirota T, Akahoshi M, Shimizu M, Tamari M, Miyatake A, et al. Coding SNP in tenascin-C Fn-III-D domain associates with adult asthma. Hum Mol Genet. 2005 ; 14 : 2779–86.
15. Moolenbeek C, Ruitenberg EJ. The "Swiss roll" : a simple technique for histological studies of the rodent intestine. Lab Anim. 1981 ; 15 : 57–9.
16. Koyama Y, Norose K, Kusubata M, Irie S, Kusakabe M. Differential expression of tenascin in the skin during hapten-induced dermatitis. Histochem Cell Biol. 1996 ; 106 : 263–73.
17. Czopka T, Von Holst A, Schmidt G, Ffrench-Constant C, Faissner A. Tenascin C and tenascin R similarly prevent the formation of myelin membranes in a RhoA-dependent manner, but antagonistically regulate the expression of myelin basic protein via a separate pathway. Glia. 2009 ; 57 : 1790–801.
18. Riddle RD, Johnson RL, Laufer E, Tabin C. Sonic hedgehog mediates the polarizing activity of the ZPA. Cell. 1993 ; 75 : 1401–16.
19. Meuronen A, Karisola P, Leino M, Savinko T, Sirola K, Majuri ML, et al. Attenuated expression of tenascin-c in ovalbumin-challenged STAT −/− mice. Respir Res. 2011 ; 12 : 2.
20. Kanda T, Nishida A, Ohno M, Imaeda H, Shimada T, Inatomi O, et al. *Enterococcus durans* TN-3 induces regulatory T cells and suppresses the development of dextran sulfate sodium (DSS)–induced experimental colitis. PLoS One. 2016 ; 11 : e0159705.
21. Agca C, Gubler A, Traber G, Beck C, Imsand C, Ail D, et al. p38 MARK signaling acts upstream of LIF-dependent neuroprotection during photoreceptor degeneration. Cell Death Dis. 2013 ; 4 : e785.
22. Greijer AE, Delis-van Diemen PM, Fijneman RJA, Giles RH, Voest EE, van Hinsbergh VWM, et al. Presence of HIF-1 and related genes in normal mucosa, adenomas and carcinomas of the colorectum. Virchows Arch. 2008 ; 452 : 535–44.
23. Midwood KS, Orend G. The role of tenascin-C in tissue injury and tumorigenesis. J Cell Commun Signal. 2009 ; 3 : 287–310.
24. Tojyo I, Yamaguchi A, Nitta T, Yoshida H, Fujita S, Yoshida T. Effect of hypoxia and interleukin-1beta on expression of tenascin-C in temporomandibular joint. Oral Dis. 2008 ; 14 : 45–50.
25. Miroshnikova YA, Mouw JK, Barnes JM, Pickup MW, Lakins JN, Kim Y, et al. Tissue mechanics promote IDH1-dependent HIF1alpha-tenascin C feedback to regulate glioblastoma aggression. Nat Cell Biol. 2016 ; 18 : 1336–45.
26. Senger DR, Galli SJ, Dvorak AM, Perruzzi CA, Harvey VS, Dvorak HF. Tumor cells secrete a vascular permeability factor that promotes accumulation of ascites fluid. Science. 1983 ; 219(4587) : 983–5.
27. Vandoorne K, Addadi Y, Neeman M. Visualizing vascular permeability and lymphatic drainage using labeled serum albumin. Angiogenesis. 2010 ; 13 : 75–85.
28. Mackie E J, Scott-Burden T, Hahn AW, Kern F, Kern F, Bernhardt J, et al. Expression of tenascin by vascular smooth muscle cells. Alterations in hypertensive rats and stimulation by angiotensin II. Am J Pathol. 1992 ; 141 : 377–88.
29. Webb CM, Zaman G, Mosley JR, Tucker RP, Lanyon LE,

Mackie EJ. Expression of tenascin-C in bones responding to mechanical load. J Bone Miner Res. 1997 ; 12 : 52-8.
30. Flück M, Tunc-Civelek V, Chiquet M. Rapid and reciprocal regulation of tenascin-C and tenascin-Y expression by loading of skeletal muscle. J Cell Sci. 2000 ; 113 : 3583-91.
31. Chiquet M, Sarasa-Renedo A, Tunç-Civelek V. Induction of tenascin-C by cyclic tensile strain versus growth factors : distinct contributions by Rho/ROCK and MAPK signaling pathways. Biochim Biophys Acta. 2004 ; 1693 : 193-204.
32. Ikeshima-Kataoka H, Shen JS, Eto Y, Saito S, Yuasa S. Alteration of inflammatory cytokine production in the injured central nervous system of tenascin-deficient mice. In Vivo. 2008 ; 22 : 409-13.
33. El-Karef A, Yoshida T, Gabazza EC, Nishioka T, Inada H, Sakakura T, et al. Deficiency of tenascin-C attenuates liver fibrosis in immune-mediated chronic hepatitis in mice. J Pathol. 2007 ; 211 : 86-94.
34. Nakahara H, Gabazza EC, Fujimoto H, Nishii Y, D'Alessandro-Gabazza CN, Bruno NE, et al. Deficiency of tenascin C attenuates allergen-induced bronchial asthma in the mouse. Eur J Immunol. 2006 ; 36 : 3334-45.
35. Wallner K, Li C, Shah PK, Fishbein MC, Forrester JS, Kaul S, et al. Tenascin-C is expressed in macrophage-rich human coronary atherosclerotic plaque. Circulation. 1999 ; 99 : 1284-9.
36. Chiquet-Ehrismann R, Chiquet M. Tenascins : regulation and putative functions during pathological stress. J Pathol. 2003 ; 200 : 488-99.